

# The growth and growth mechanism of lithium tetraborate

D. S. ROBERTSON, I. M. YOUNG

Royal Signals and Radar Establishment, Malvern, Worcs, UK

The conditions required to grow high quality lithium tetraborate single crystals are described, along with the defects likely to be encountered during growth of the crystals. The relationship of the latter to the growth mechanism is discussed and a mechanism proposed which provides an explanation of the observed nature of the defects and of the manner in which the crystals grow and reject impurities.

## 1. Introduction

Single crystals of lithium tetraborate were first produced by Garrett *et al.* [1] for use in infra-red transmission studies. Recently, crystals of this compound have been shown to exhibit interesting piezo-electric properties [2]. These properties make them attractive for surface acoustic wave device applications. The work below reports the results obtained during a study of the growth of such crystals and the relationship of these results to the crystal growth mechanism.

## 2. Experimental procedure

The crystals were grown by the vertical lift technique (Czochralski technique) using equipment previously described [3]. The melts were prepared by melting samples of the borate obtained earlier by direct reaction of the relevant components or as lithium tetraborate from commercial sources. The melts were contained in platinum crucibles of either 50 mm diameter and 50 mm depth or 75 mm diameter and 75 mm depth. Both radio-frequency heating and resistance element heating were used.

The growth rates used ranged between 0.5 mm h<sup>-1</sup> and 3.0 mm h<sup>-1</sup>. Crystal rotation rates in the range 4 to 40 rpm were investigated, along with different flowing and static gas ambients and crystal growth axes.

## 3. Results and observations

Contrary to the results given by Garrett *et al.* [1], no difficulties were experienced using platinum

crucibles to contain the melt. The pure melts are completely transparent. As a result, fluid movement is not observed. However, the addition of dopants produces opaque melts and fluid cell patterns and fluid movement are made apparent. Both the *x* (100) and *z* (001) axes were used as growth directions. The crystals formed are transparent and colourless. However, a major difficulty encountered during the growth of the crystals, shown in Figs 1 and 2, is the formation of cores and defect regions which consist largely of opaque inclusions. Such a region is shown, at higher magnification, in Fig. 3. The pattern of distribution across the crystal diameter was sometimes related to changes in crystal diameter which occurred during growth but was more often like that shown in Fig. 1 where there was no strong relationship and where, like the cores previously described in cadmium tungstate [4], the origin of the core was always at the centre of the crystal.

Coring as described was encountered in both (100) and (001) crystals and was unaffected by changes in rotation rate up to rotation rates of 40 rpm. Above this rotation rate the crystal growth became unstable and the crystal grew dendritic protuberances. Changes in gas ambient from oxidizing (air) to neutral (nitrogen or argon) also had no effect on the cores or the colour of the crystals. As a result, the selected rotation rate was 5 rpm and the selected growth ambient was static or flowing air.

The factors which did affect the cores were the growth rate, the period of growth and the

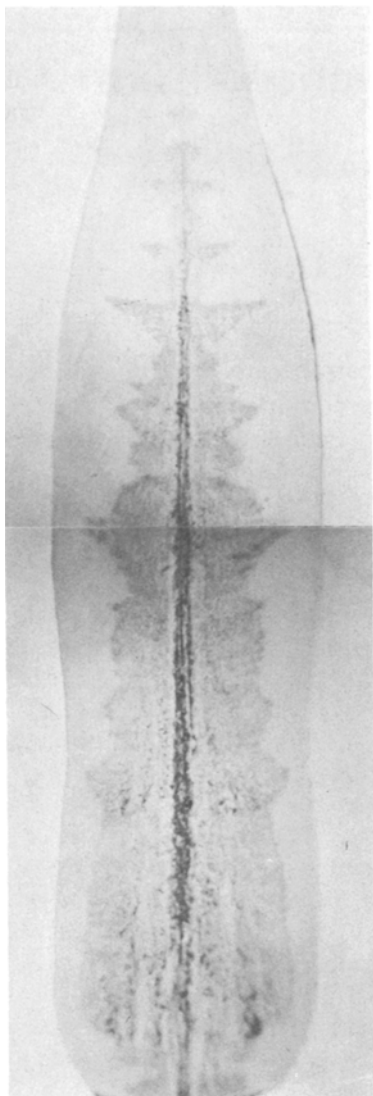


*Figure 1* A section along a  $\langle 001 \rangle$  crystal of lithium tetraborate showing core defect ( $\times 1.6$ ).

preparation of the starting material. For all starting materials a growth rate in excess of  $2 \text{ mm h}^{-1}$  could not be sustained without the cored region encompassing virtually all the crystal. At high growth rate and at a growth rate of  $< 1 \text{ mm h}^{-1}$  from inferior quality material the crystal diameter decreased and separated from the melt. This happened even when no temperature changes were made. Using the best starting material and a growth rate of  $0.5 \text{ mm h}^{-1}$  cores tended to seriously affect the crystal quality only after about fifty per cent of the melt had been converted to single crystal, that is, after a period of about three days.

Lithium tetraborate can be prepared by several

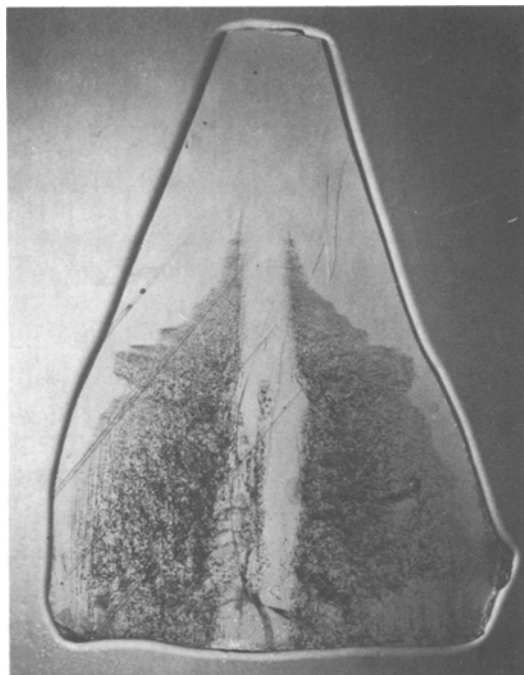


*Figure 2* A section along a  $\langle 100 \rangle$  crystal of lithium tetraborate showing split core defect ( $\times 3.2$ ).

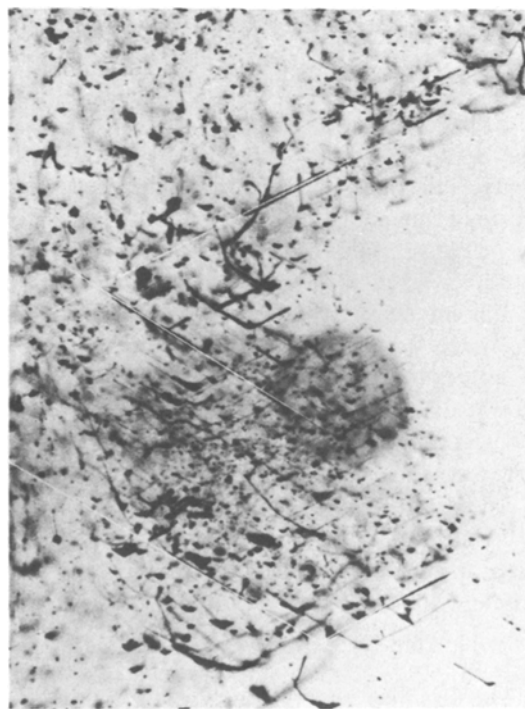


*Figure 3* Magnified core defect of lithium tetraborate crystals ( $\times 365$ ).

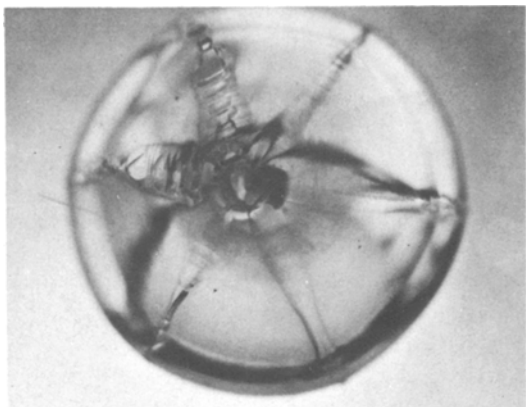


Figure 4 The top of a  $\langle 100 \rangle$  lithium tetraborate crystal.

methods. These are: by reaction of lithium hydroxide and boric acid in solution followed by evaporation to dryness, by reaction of lithium nitrate and boron trioxide above  $600^\circ\text{C}$ , by reaction of lithium carbonate and boron trioxide above  $600^\circ\text{C}$  and by the latter reaction but taking precautions to ensure decomposition of the carbonate, as was performed by previous workers [1]. Only the latter two reactions produce material which is suitable for growth. However, even with this material, cores could appear in crystals and it was observed that after growth the melts which had started as transparent solids had become opaque. Opaque starting material was also sometimes obtained during the preparation of the material. Two samples of borate crystal were chemically analysed, one with a slight core and the other core-free. The analysis showed that the cored crystal had a higher lithium content than the core-free material. Debye-Scherrer X-ray powder diffraction photographs of the cored material showed faint extra lines over those attributable to lithium tetraborate. These extra lines were also present and stronger in the X-ray powder photograph of a residual melt and shown to correspond to lithium metaborate ( $\text{LiBO}_2$ ). Commercially-available electronic grade lithium tetraborate also shows faint lithium metaborate lines in its powder photograph. After a crystal growth run had been completed, there was always a white deposit on the walls of the growth chamber implying a loss of material from the melt. This deposit was found to be crystalline and the powder photograph obtained gave a set of  $d$ -spacings corresponding to  $\text{Li}_2\text{O}\cdot 5\text{B}_2\text{O}_3\cdot \text{H}_2\text{O}$ , as identified by Sastry and Hummel [5]. Whether this compound evaporates

congruently from the melt or the components react in the gaseous state in the growth chamber is uncertain, but the differential thermal analysis (DTA) of the material confirms its composition to be  $\text{Li}_2\text{O} : \text{B}_2\text{O}_3$  1 : 5, implying that  $\text{B}_2\text{O}_3$  is being lost at five times the rate of  $\text{Li}_2\text{O}$ . The total loss of material during a growth run is, however, only about 0.5 %.

The chemical analysis of the two samples also showed that the ratio  $\text{B}_2\text{O}_3 : \text{Li}_2\text{O}$  in both cored and core-free material was higher than the theoretical ratio, being 68.9 mol%  $\text{B}_2\text{O}_3$  for the core-free material as opposed to the theoretical 66.6 mol%  $\text{B}_2\text{O}_3$ .

Investigations of the additions of excess lithium carbonate and excess boric oxide during both starting material preparation and growth of crystals established that preparation or growth with lithium-rich compositions with a lithium excess as low as 0.1 mol% were detrimental. On the other hand, preparation and growth with boron trioxide at 1.0 mol% excess reduced coring and produced better quality crystals.

Both  $\langle 100 \rangle$  and  $\langle 001 \rangle$  crystals, though nominally circular in cross-section, have prominent external features. The former shows three pairs of nearly equi-spaced fins, as shown in Fig. 4. When viewed along the growth direction one pair are parallel to the  $[010]$  axis and the other two pairs are inclined at  $29^\circ$  to the  $[001]$  axis. The crystal with  $\langle 001 \rangle$  growth direction, when viewed along this direction, shows four major fins (Fig. 5) in the  $\langle 110 \rangle$  series of directions and four minor fins equi-spaced between the major fins. In both crystals during the growing-out period, minor facets develop on four of the

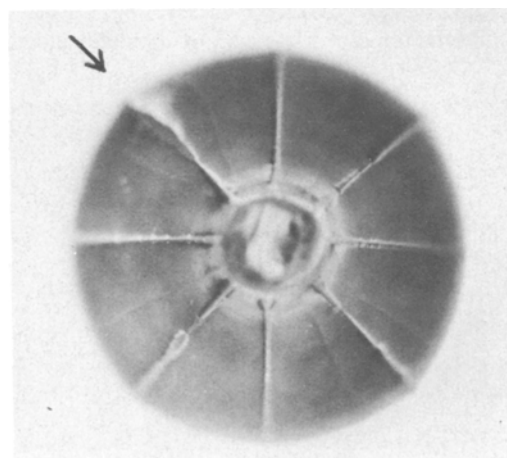


Figure 5 The top of a  $\langle 001 \rangle$  lithium tetraborate crystal.

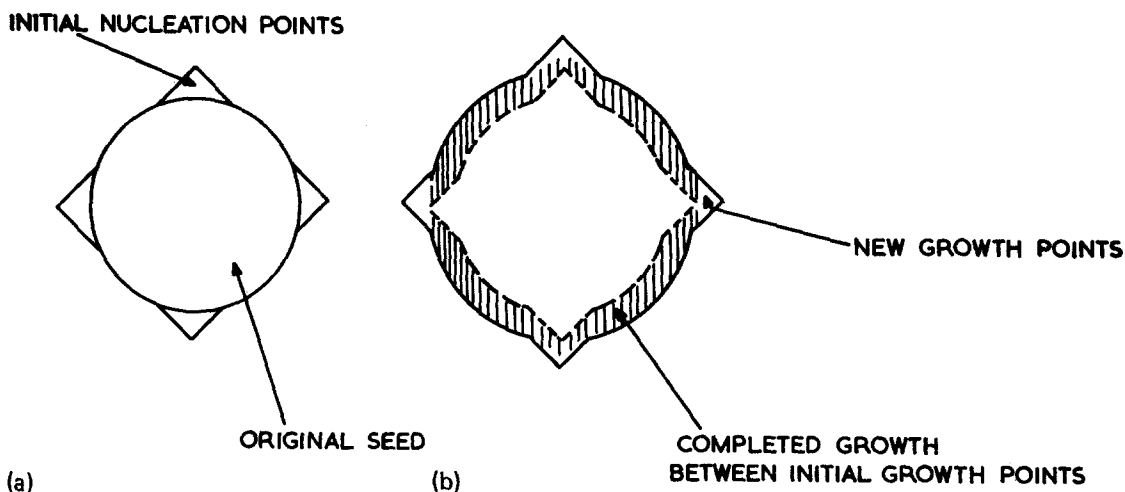


Figure 6 A diagrammatic representation of the observed growth outwards over the liquid surface of lithium tetraborate crystals.

fins. In the case of the  $\langle 100 \rangle$  crystal, optical examination shows the facet normal to be at about  $65^\circ$  to the growth axis on the fins at  $29^\circ$  to the  $\langle 001 \rangle$  direction. In the case of the crystal with  $\langle 001 \rangle$  as growth direction where growth-out has been fairly rapid, facets are observed on the four major fins, the facet normal being about  $38^\circ$  to the growth axis. After shouldering when this crystal is growing nominally parallel, the four major fins become more pronounced being bounded by two mutually orthogonal faces the intersection of which is  $[001]$ . This external ridge has a serrated appearance, being broken in places by microfacets parallel to those observed during growth-out. When a  $\langle 100 \rangle$  crystal is growing parallel the pair of fins parallel to  $[010]$  also show a slight tendency to facet and if this crystal is decanted rapidly from the melt a central faceted region of interface is observed, (see Fig. 7).

Observations of the stages of diameter increase

showed that in the case of  $\langle 001 \rangle$  crystals, growth commences at the four junctions of the  $\{100\}$  planes (see Fig. 6a). Growth is then completed to join these and the four junctions once again form (see Fig. 6b) and the process is repeated. In both  $\langle 100 \rangle$  and  $\langle 001 \rangle$  crystals when the crystal degrades through the presence of a core, the nature of the cellular structure that results is related to the external morphology. Fig. 7 shows three stages of degradation of a  $\langle 100 \rangle$  crystal viewed perpendicular to the growth axis. Fig. 2 shows a longitudinal section of a similar crystal. What is apparent from Fig. 2, and is not obvious when examining a complete crystal, is that the core is split and starts from two distinct points near the centre of the crystal. The central region of the crystal remains core-free over much of the length of the crystal even though the defect region is spreading outwards. The nature of the coring appears linear and at first slightly radial,

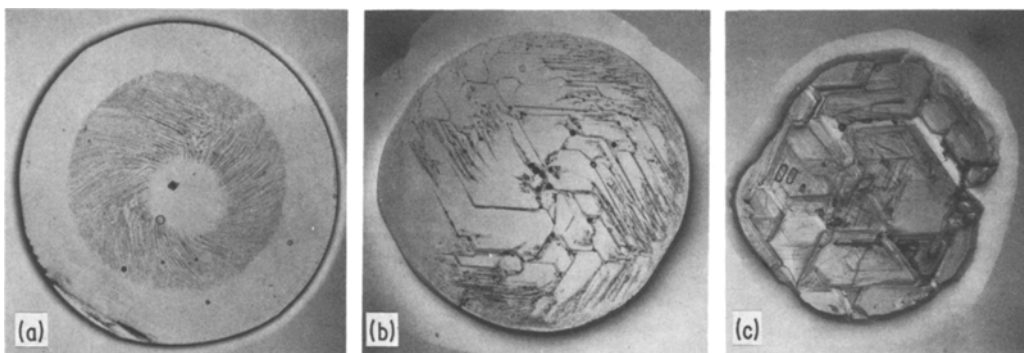


Figure 7 Progressive break-down of a  $100$  interface.

though there is some preferred orientation which becomes more evident as the affected area of crystal becomes larger (see Fig. 7c). A Laue X-ray back-reflection photograph shows that the [010] and [001] axes of the crystals lie along the short and long diagonals, respectively, of the diamond-like array of micro-cracks. Fig. 7c shows the end of a crystal where complete interface break-down has occurred and the crystal is growing in a number of large faceted cells over the entire interface. The cell walls can be seen to have generally the same diamond appearance noted in Fig. 7b, being  $61^\circ$  to the [001] direction, though there are a number of cell boundaries lying parallel to [001]. A closer investigation of the structure of the core regions shows the linear features to contain material with no defined morphology but appearing as globular aggregates.

The degradation of a [001] crystal is slightly different and is shown in Fig. 8. In a thin section perpendicular to the growth axis a linear structure to the core is again observed with a preferred orientation but in this case a square array is observed, the [100] and [010] directions being the square diagonals. Unlike the  $\langle 100 \rangle$ -grown crystal, the core even at its early stages affects the central region of the crystal and progressively

encompasses the whole of the growing interface (see Fig. 8b). The degradation here has not quite reached the stage of the  $\langle 100 \rangle$  crystal shown in Fig. 7c but if growth is continued a square pyramidal-cell structure is seen to have developed. As in the case of the  $\langle 100 \rangle$  crystal where, the diamond-like structure of the core section is modified to include triangular cells, so the square structure of the  $\langle 001 \rangle$  crystal core becomes modified as degradation proceeds. In this case, a second square array becomes interlaced with the original, the latter being displaced by  $45^\circ$  to the former. A closer examination of Fig. 8b shows alternating areas of linear arrays. These arrays are curviform in nature and give the core a whorled effect. The direction of the whorl when viewed from the top of the crystal is counter to the direction of rotation of the crystal. Fig. 1 is a longitudinal section of a  $\langle 001 \rangle$  crystal viewed along the [100] direction showing its irregular banded appearance. The shape of the top of the band is presumably related to the interface shape and that of the lower edge is related to the preferred orientation of the defect structure, as shown in the magnified section of a band seen in Fig. 3. These lie at about  $60^\circ$  on either side of the  $\langle 001 \rangle$  growth axis.

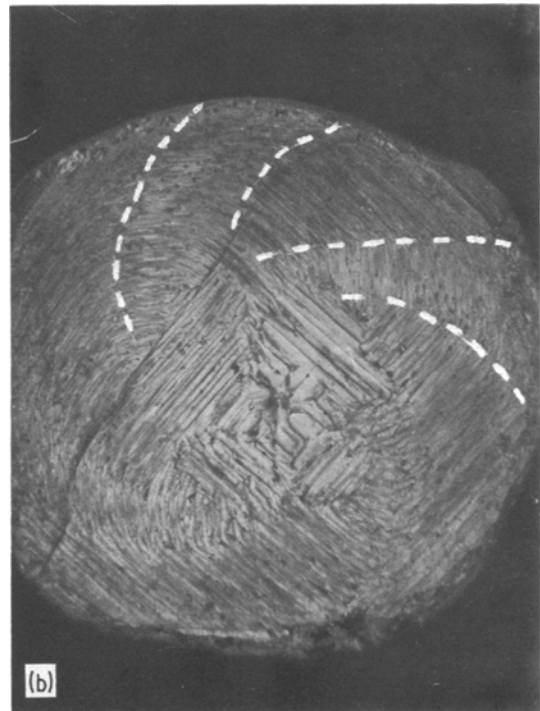
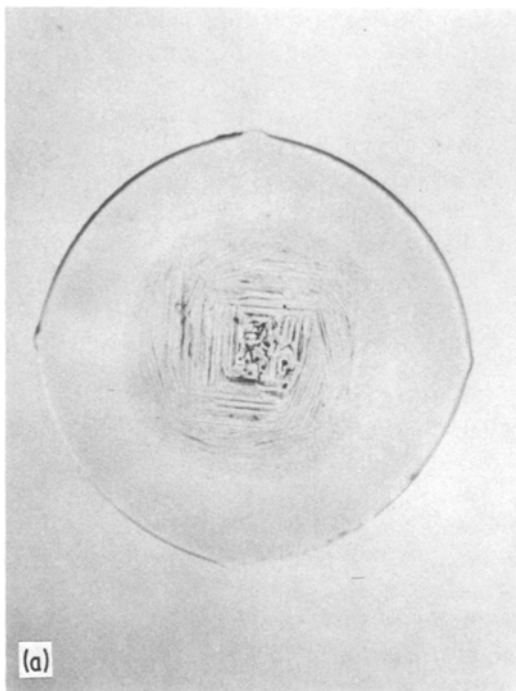


Figure 8 Progressive break-down of a 001 interface.

#### 4. Discussion

Good quality lithium tetraborate single crystals can be prepared by growth from the melt at rotation rates of 5 rpm and at a growth rate of  $< 1.0 \text{ mm h}^{-1}$  from boron trioxide-rich starting material in an ambient of air either static or flowing. The major fault encountered during growth is the presence of cores. These cores, like those previously observed [4] in cadmium tungstate, originate at the centre of the crystal and can spread out through the entire crystal, as described above. They are composed of lithium-rich material and could be lithium hydroxide or carbonate impurity originating from the borate preparation method. They could also be lithium oxide resulting from the fact that boron trioxide is predominantly lost from the melt during growth. There is no doubt that the former two impurities can be involved from the evidence presented. However, even when they have been eliminated the cores persisted.

From the X-ray powder diffraction data the core region is seen to consist of lithium metaborate and is, hence, lithium-rich with respect to the bulk of the crystal. This is confirmed by the chemical analysis. The excess lithium could arise from incomplete reaction of starting materials. It was noticeable that opaque starting melts gave more serious coring. This was true even with fully-reacted material commercially available. This material however always contained a small percentage of metaborate and implies the presence of an equal amount of free boric oxide to give the analytical result. It was not possible to positively identify this phase in the powder photograph of the starting material and, indeed, if the boric oxide was present as a glass it would be undetectable. The possibility is that the compensating boron phase is  $\text{HBO}_2$  this is a highly stable species and has been detected in the vapour up to  $1178^\circ \text{C}$ . However, it is unlikely that such species exist as separate entities in the molten material.

There thus remain two possibilities concerning the origin of excess lithium oxide. The first is that the maximum melting point of the material which crystallizes is not at the 1 : 2 mole ratio taken from the diagram by Sastry *et al.* [5]. Such a situation is analogous to that observed for lithium tantalate or niobate [6]. In the case of the lithium borate the maximum melting point would be on the boron trioxide-rich side of the

1 : 2 mole ratio. Although there is nothing in the phase diagram [5] to indicate this, there is no reason why such a situation should have been detected since the evidence from this work indicates the deviation is only 1 or 2 mol%.

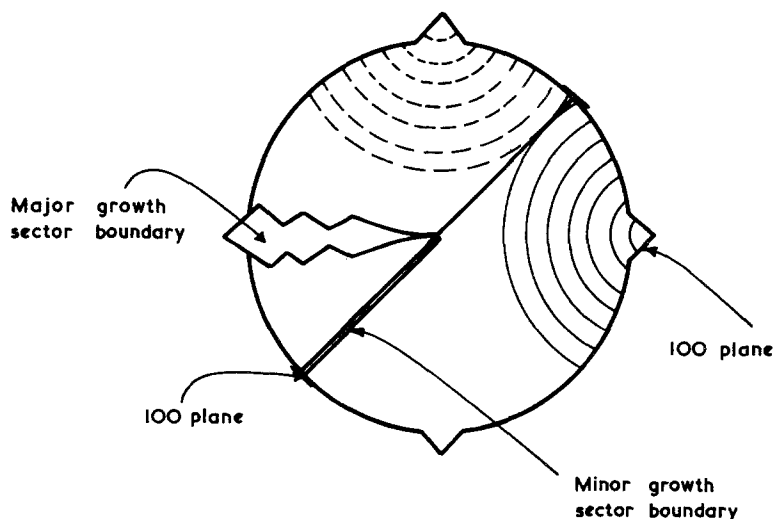
The second source of lithium oxide excess is preferential loss of boron trioxide from the melt. The results showed that this was a very small fraction of the total weight. However, these melts are quite viscous (247 with respect to water at  $25^\circ \text{C}$ ) and loss of boric oxide from the surface regions in contact with and near to the growing crystal could take such a long period to be balanced by fluid flow (thermal or hydrodynamic) or diffusion that substantial lithium oxide accumulation at the interface is the result. The first of the two possibilities has been previously observed and thus must be the most likely reason for core formation in crystals grown from reaction product-free material. The accumulation of excess lithium oxide at the interface causes a lowering of the melting point of material in this region. If adjustments are made to the temperature the crystal diameter will remain constant but the material which tends to crystalline will be lithium metaborate which melts at  $815^\circ \text{C}$ . If no adjustments to temperature are made then the crystal diameter will decrease and the crystal will ultimately separate from the melt, as observed.

As in the case of cores in previous crystals [4] the origin of the coring at the centre of the growing interface implies that impurity accumulation first reaches a concentration sufficiently high at this point to interfere with growth. In the case of  $\langle 100 \rangle$  crystals a definite facet was observed along with the distribution of a higher concentration of impurity off the facet. It was also observed that the spread of the impurity across the interface was not necessarily related to changes in external shape.

All of the observations are related to the manner of growth from the melt and particularly to the rejection of impurities by the growing crystal. There is no doubt that impurity accumulation causes the cores in the manner postulated by Tiller [7] and developed by others [8]. However, the impurity distribution across a growing interface is clearly not uniform in terms of concentration.

Discussions of the process of impurity removal from a growing interface postulate rejection of the impurity into a diffusion-dominated region in contact with the interface. These discussions

Figure 9 The proposed origins of crystal growth.



further consider that the diffusion away from the interface is everywhere principally directed in a direction normal to the interface. Such a situation would not result in the non-uniformity of impurity distribution observed in lithium borate crystals. This non-uniformity of impurity distribution could arise as a result either of the growth process or of the fluid movement at the interface. Because fluid movement at the interface is zero, the attainment of the highest impurity concentration at a particular point is unlikely to arise from this cause.

Thus, the growth mechanism must be involved. A model which would explain the observations is as follows. Fig. 9 is a diagrammatic representation of the  $\langle 001 \rangle$  crystal shown in Fig. 4. The major growth sector boundaries at the periphery of the crystal which are the junctions of the  $\{100\}$  planes and the flat regions at the periphery which form at the ends of the minor growth sector boundaries are also  $\{100\}$  planes. Thus, as Fig. 9 shows, the cross-section shape of  $\langle 001 \rangle$  crystals if fully developed would be square. It is proposed that growth is initiated at the junctions of the  $\{100\}$  planes since they represent a region of high defect concentration or high strain, as they do in crystals such as quartz and KDP. It is considered that nucleation is induced by the passage of these junctions through one of the fluid cell walls which exist in the melts and are cooler regions [9]. From these points, sheets of crystallizing material spread downwards and inwards towards the centre of the interface in a manner similar to that proposed by Chernov and others [10, 11, 16]. Crystallizing species form in these sheets by

addition at the stepped edge of the sheet. The thickness of these sheets need only be one unit cell thick and where sheets intersect growth sector boundaries form. This mechanism is supported by the similarity of form of major growth sector boundary formed by the intersection of the fronts on the diagram (Fig. 10) and that of the actual growth sector boundary (shown arrowed in Fig. 5). It is further supported by the orientation of the rectangle of the area where interface break-down

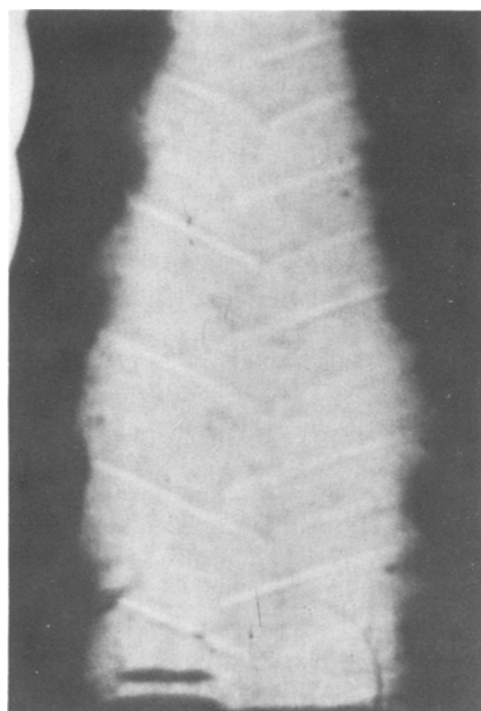


Figure 10 Interlocking sheets in a lithium niobate crystal.

has occurred, as shown in Fig. 8a. Since it might be expected that growth sector boundaries could be identified in the interior of the crystal, and since this was not confirmed by X-ray, optical or chemical methods, it is proposed that visible boundaries only formed at free surfaces, and that sheets do not nucleate simultaneously at all four  $\{100\}$  plane junctions but nucleate sequentially. In this case they would pass over each other at the interface centre in an interlocking manner. Such a postulation is supported by Fig. 10 where an interlocking effect is shown in a crystal of lithium niobate grown in this laboratory.

From the observations on the external morphology and a consideration of the structure of lithium tetraborate, as determined by Krogh-Moe [12, 13], it is apparent that the  $\{112\}$  planes are forming the observed exterior angled facets in the case of (001) crystals and the  $\{100\}$  planes are forming the facet normal to the growth axis for (100) crystals. The pyramidal cell structure in both crystals is thus formed by four  $\{112\}$  planes; but, in the case of the  $\langle 100 \rangle$  crystals the pyramids are truncated by the  $\langle 100 \rangle$  facet perpendicular to the growth direction. Based on this observation, it is proposed that the sheets of crystallizing material are in fact  $\{112\}$  planes in the case of (001) crystals and that the functions of these four planes are the growth sector boundaries. The advance of the  $\{112\}$  sheet edges is limited by the position of the melting-point isotherm, see Fig. 11.

A similar mechanism operates in the  $\langle 100 \rangle$  crystals, except that on this interface there is another junction between planes giving another growth sector boundary which defines the facet shown in Fig. 11. Growth on this facet is considered to proceed by either independent nucleation at the latter boundary or by nucleation initiated by a  $\{112\}$  sheet reaching this junction, the sheet edges moving towards the facet centre. The presence of a central defect in the form of a hole in the facet supports this model of sheet movement on the  $\langle 100 \rangle$  facet. This model invokes physical movement at the interface (Fig. 11) as a result of the sheets passing through the fluid. At the interface, fluid movement will be induced and a trailing flow of liquid will form. This will contain both crystallizing species and non-crystallizing species (impurity). To obtain the likely relative concentrations of these species, from the periphery where the crystallizing sheets originate to the centre where they meet, an adaptation

of the Wagner analysis [14, 15] of species depositing from a fluid streaming over a plane surface can be used. The expression has the form

$$\frac{C}{C_0}(x, t) = 1 - \frac{2K D x}{(\pi)^{1/2} h v 2(D t)^{1/2}}, \quad (1)$$

where  $C_0$  is the initial concentration in the stream,  $C$  is the concentration at some point along the surface after time  $t$ ,  $v$  is the velocity of the stream,  $h$  is the height of the stream,  $D$  is the diffusion coefficient into the surface and  $K$  is the ratio of depositing species in the surface to that in the fluid stream. Low values of  $K$  encourage growth. The derivation makes the assumptions that the concentration of depositing species in the fluid is not affected by any diffusion normal to the plane and, further, that diffusion into the surface is very small. In applying this expression to the growth of lithium borate these two assumptions are reasonable since, first, if diffusion normal to the sheets forming along  $\{112\}$  planes were dominant, then the non-uniform distribution observed could not occur, and second, it is evident that the crystallizing species do not diffuse into the growing surface but attach to it.

Thus, the  $K$  factor is the same as for the derived conditions,  $D$  is identified with the surface diffusion coefficient of the Burton, Cabrera and Frank nucleation theory [16],  $h$  is the height of the growth-induced flow, and defined as the distance from the growing sheets where the velocity of this flow,  $v$ , equals that of thermal or hydrodynamic fluid flow in the liquid.

On reaching the periphery of the crystal, deposition of the lithium tetraborate species begins and the grow-induced flow commences. After time  $t$  at some point  $x$  removed from the periphery the concentration of lithium borate species in the growth-induced flow will have decreased and, conversely, the non-crystallizing species (impurity) will have increased. Thus, the impurity is increasing towards the centre of the crystal.

This result evidently explains the build-up of impurity to a level which causes the interface to break down in a manner treated by Tiller *et al.* [7] and Hurle [8] at the centre of  $\langle 001 \rangle$  crystals.

The situation for  $\langle 100 \rangle$  crystals is complicated by the fact that two growth-induced flows form, as shown in Fig. 11. These are considered dependent on one another only to the extent that the arrival of a  $\{112\}$  sheet edge at the



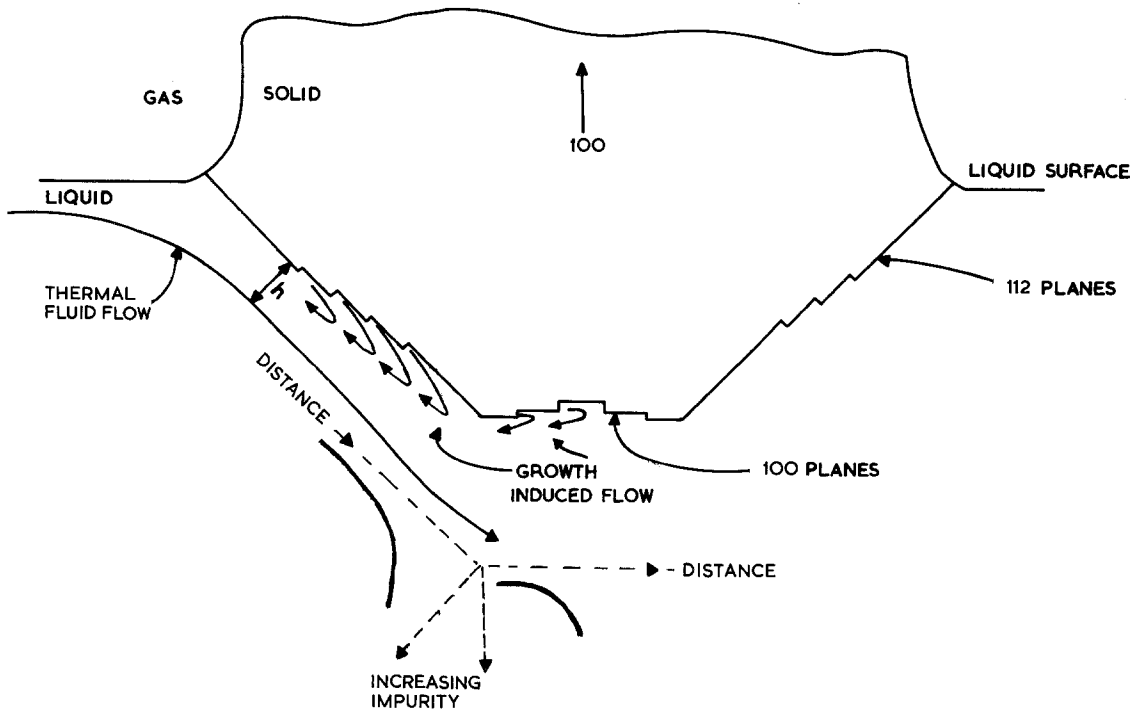


Figure 11 The proposed flows at the liquid–solid interface.

junction initiates a sheet on the  $\{100\}$  planes. The abrupt nature of the interface break-down between the  $\{112\}$  and  $\{100\}$  planes, shown in Fig. 4, supports this conclusion. On this basis, the rate of increase of impurity need not be the same parallel to the  $\{100\}$  planes as parallel to the  $\{112\}$  planes. The Wagner expression modified as described indicates this since, in the first instance, the surface diffusion coefficient,  $D$ , will not be the same and, in the second instance, the value of  $h$  will change because the thermal flow, while it may be parallel to the  $\{112\}$  planes, cannot be parallel to  $\{100\}$  planes at the same time. Thermal flow

from observations of the doped lithium borate melts is from the crucible walls towards the periphery of the crystal and then downwards towards the crucible base. It is the dominant flow due to the low rotation rate used and the high melt viscosity [17]. Such a flow would, hence, only have a component parallel to the  $\{100\}$  planes. This means a reduced velocity in this direction leading to a change in  $h$  which, in turn, affects the Wagner distribution over the length of the plane involved. The presence of independent Wagner flows is supported by the distribution of defects shown on the X-ray topo-

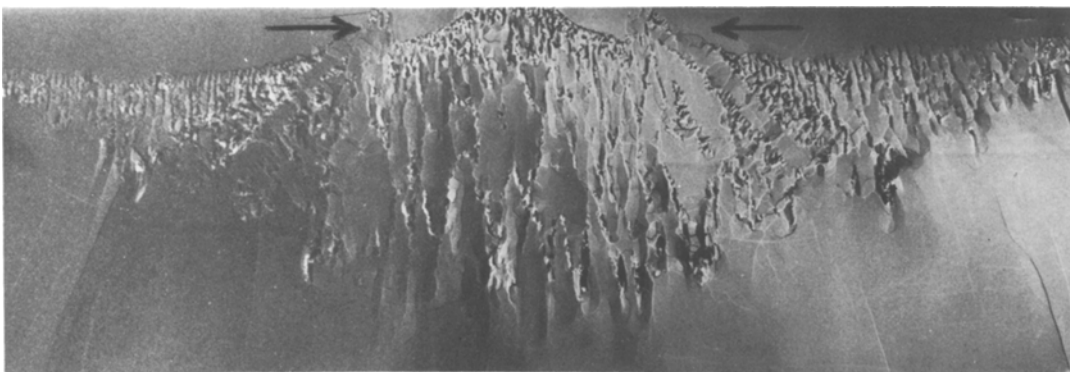


Figure 12 Defects aligned in the form predicted by the Wagner analysis in a lithium niobate crystal. (Courtesy Barr and Stroud Ltd, Glasgow, UK.)

graph of part of a lithium niobate crystal, shown in Fig. 12.

Thus, the build up of impurities at the centre of the {100} face would be expected to lead or lag behind that of the {112} faces and, hence, interface break-down would occur sooner or later than on the {112} face. From Fig. 2, showing the split core effect, it is evident that the interface break-down lags on the {100} planes because it begins later on this face.

## 5. Conclusion

It has been shown that high-quality lithium tetraborate single crystals can be grown from the melt. A model has been developed which proposes that a growth-induced fluid flow exists at the solid-liquid interface. This has been used to explain the non-uniformity of impurity distribution observed from defects in these crystals.

## Acknowledgements

This paper is published by permission of the © Copyright Controller, H. M. Stationary Office, London.

## References

1. J. D. GARRETT, M. NATARAJAN-IYER and J. E. GREEDAN, *J. Cryst Growth* 41 (1977) 225.
2. R. W. WHATMORE, N. M. SHORROCKS, C. O'HARA, F. W. AINGER and I. M. YOUNG, *Elect. Lett.* 17 (1981) 11.
3. B. COCKAYNE, D. S. ROBERTSON and W. BARDSLEY, *Brit. J. Appl. Phys.* 15 (1964) 1165.
4. D. S. ROBERTSON, I. M. YOUNG and J. R. TELFER, *J. Mater. Sci.* 14 (1979) 2967.
5. B. S. R. SASTRY and F. A. HUMMEL, *J. Amer. Ceram. Soc.* 41 (1958) 7.
6. P. LERNER, C. LEGRAS and J. P. DUMAS, *J. Cryst. Growth* 3 (1968) 231.
7. W. A. TILLER, K. A. JACKSON, H. W. RUTTER and B. CHALMERS, *Acta. Met.* 1 (1953) 428.
8. D. T. J. HURLE, *Solid Stat. Elect.* 3 (1961) 37.
9. B. COCKAYNE and M. P. GATES, *J. Mater. Sci.* 2 (1967) 118.
10. A. CHERNOV, *J. Cryst. Growth* 24/25 (1974) 11.
11. T. ABE, *ibid.* 24/25 (1974) 463.
12. J. KROGH-MOE, *Acta Cryst.* 15 (1962) 190.
13. *Idem*, *ibid.* B24 (1968) 179.
14. C. WAGNER, *Z. Phys. Chem.* A192 (1943) 157.
15. *Idem*, *J. Mater. Sci.* 16 (1981) 413.
16. K. W. BURTON, N. CABRERA and F. C. FRANK, *Phil. Trans. Roy. Soc.* A866 (1951) 243.
17. D. S. ROBERTSON, *Brit. J. Appl. Phys.* 17 (1966) 1047.

*Received 30 September  
and accepted 9 November 1981*